HISTORICAL BIOLOGY
https://doi.org/10.1080/08912963.2024.2408617

Taylor & Francis
Taylor & Francis Group

Post-cranial remains of Rhinocerotidae from the Neogene of central Myanmar: morphological descriptions and comparisons with ratios

Morgane Longuet[a], Naoto Handa[b], Zin-Maung- Maung-Thein[c], Thaung- Htike[d], Man-Thit- Nyein[e] and Masanaru Takai[f]

[a]The Kyoto University Museum, Kyoto University, Inuyama, Aichi, Japan; [b]Lake Biwa Museum, Kusatsu, Japan; [c]Department of Geology, University of Mandalay, Mandalay, Myanmar; [d]Department of Higher Education, Naypyitaw, Myanmar; [e]Division of World Heritage Site, Pyay, Myanmar; [f]The Kyoto University Musem, Kyoto University, Kyoto, Japan

ABSTRACT

New post-cranial remains from the early Late Miocene have been discovered in the lowermost part of the Irrawaddy Formation, Tebingan area, central Myanmar. Three genera and one indeterminate taxon were identified: *Rhinoceros* sp. *Rhinoceros* cf. *R. sondaicus*, *Dicerorhinus* sp., *Brachypotherium perimense*, and Rhinocerotidae indet. The evolutionary history of the Rhinocerotidae is still poorly known in Southeast Asia. Few *Rhinoceros* species, *Rhinoceros* sp. '*B*'. *fatehjangense*, and *B. perimense*, has already been identified in the Tebingan area by dental remains. The present discovery of the post-cranial remains of *Rhinoceros* cf. *R. sondaicus* and *Dicerorhinus* sp. that complements previous studies based on dental remains. The early Late Miocene Tebingan record is the oldest fossil record of *Dicerorhinus* in Southeast Asia, indicating a continental origin of the genus. Furthermore, the possible presence of *R. sondaicus* in the Tebingan area suggests that it may have appeared in Southeast Asia as early as the early Late Miocene.

ARTICLE HISTORY
Received 7 December 2023
Accepted 18 September 2024

KEYWORDS
Rhinocerotidae; Irrawaddy Formation; Myanmar; Neogene; paleobiogeography; southeast Asia

Introduction

The Rhinocerotidae family was widely distributed between the Eocene and Pleistocene in Eurasia, North America, and Africa (Antoine et al. 2003). Today, it is represented only in South/Southeast Asia and Africa by four genera and five species (Nowak 1991). The family reached its apogee at the beginning of the Neogene, with a great diversity of genera and species (Prothero et al. 1989; Heissig 1999; Antoine 2002; Prothero and Schoch 2002). The Rhinocerotidae became extinct in North America after the Pliocene. At the same time, the Rhinocerotina, including *Rhinoceros*, *Dicerorhinus*, *Ceratotherium*, and *Diceros*, remained and Africa up to the present day (Prothero 2005). Many Neogene Rhinocerotidae fossils have been identified in South Asia, demonstrating their diversity in this geological period (Geraads et al. 2021; Antoine et al. 2022); however, their evolutionary history is still poorly known.

Located in central Myanmar, the Tebingan area has yielded several cranial fossils (mainly isolated teeth) related to: *Rhinoceros* sp., *Brachypotherium perimense*, and '*B.*' *fatehjangense*. *Brachypotherium*, a hornless rhinoceros that lived in forest or wooded environments and possibly in semi-aquatic habitats (Handa et al. 2018; Rafeh et al. 2020), is known from the late Early to early Late Miocene in Europe. At the same time, it survived until the Late Miocene at Lothagam (Geraads 2010) and at Sahabi (Libya) in Africa with *B. lewisi* (Pandolfi and Rook 2019). Furthermore, an undetermined brachypothere has been found in the Pliocene of Congo (Geraads 2010). *Brachypotherium* appeared during the late Middle Miocene in Pakistan (Chinji Formation, Siwalik), Myanmar (Irrawaddy sediments), and Thailand (Nakhon Ratchasima) (Antoine et al. 2013; Handa et al. 2021; Longuet et al. 2023).

Rhinoceros is known from the Late Miocene until the Pleistocene in Pakistan, Myanmar, Indonesia, China, and Thailand (Khan 2009; Métais et al. 2009; Zin-Maung-Maung-Thein et al. 2010; Antoine 2012). The presence of this genus in Myanmar during the early Late Miocene shows dispersal from the Indian subcontinent to Myanmar during the Late Miocene due to environmental changes that occurred in the Siwalik Group around 10.3 Ma (Cerling et al. 1997; Longuet et al. 2023). In addition, the coastline retreat to southern Myanmar gave way to humid, closed environments favorable to Rhinocerotidae (Zin-Maung-Maung-Thein et al. 2011; Habinger et al. 2022). This genus is currently known by two modern species, *R. unicornis* (Indian rhinoceros) from the Himalayan foothills, excluding the Indochina region, and *R. sondaicus* (Javan rhinoceros) from the western end of Java (Laurie et al. 1983; Groves and Leslie 2011).

To date, numerous rhinocerotid fossils have been discovered in Neogene sediments, most of which have been identified by craniodental remains (mandible, maxilla, and isolated teeth) (Chavasseau et al. 2006; Zin-Maung-Maung-Thein et al. 2010; Longuet et al. 2023). Very few post-cranial remains have so far been examined in detail. In this study, we describe several post-cranial remains of rhinocerotids discovered in the lowest strata of the Irrawaddy Formation in the Tebingan area, central Myanmar, providing further evidence of rhinocerotid distribution in the late Miocene of Myanmar.

Geological settings

Dating from the early Late Miocene to the Early Pleistocene, the Irrawaddy Formation consists of non-marine sediments widely exposed along the Ayeyarwady (=Irrawaddy) and Chindwin rivers. It is subdivided into lower and upper parts based on palaeontological and lithological criteria (Stamp 1922; Bender 1983). The mammalian fauna from the lower part of the Irrawaddy Formation is comparable to the Middle Siwalik Nagri (11.5–9 Ma) and Dhok Pathan (9.8– ca. 3.5 Ma) Formations of the Middle

CONTACT Morgane Longuet longuet.morgane9@gmail.com The Kyoto University Museum, Kyoto University, 41 Kanrin, Inuyama, Aichi 484-8506, Japan
Supplemental data for this article can be accessed online at https://doi.org/10.1080/08912963.2024.2408617.

Published online 07 Oct 2024

Siwalik, corresponding to the early Late Miocene to the Early Pliocene (Zin-Maung-Maung-Thein et al. 2011; Takai et al. 2015), while the upper Irrawaddy fauna is comparable to the Upper Siwalik, dating from the Late Pliocene to the Early Pleistocene (Colbert 1943; Bender 1983) (Figure 1).

In the Tebingan area, the fluvial Irrawaddy Formation conformably overlies the shallow marine Obogon Formation (Middle Miocene) of the Pegu Group (Takai et al. 2021). Most of the Tebingan vertebrate fossils have been collected from the lowermost part of the Irrawaddy Formation or the upper parts of the Obogon–Irrawaddy transition zone. The geological age of the Irrawaddy Formation in Tebingan is estimated from the combination of several mammal genera, with a well-established chronological distribution in the Siwalik deposits (northern Pakistan), suggesting an early Late Miocene age (9–8 Ma) (Barry et al. 2002; Takai et al. 2021). This age is supported by the faunal composition of the Tebingan area with the presence of *Hipparion* cf. *theobaldi* (Equidae, Perissodactyla), *Anisodon* sp. (Chalicotheriidae, Perissodactyla), *Bramatherium megacephalum* (Giraffidae, Artiodactyla), and *Hippopotamodon sivalense* and *Tetraconodon* spp. (Suidae, Artiodactyla), as well as by the absence of *Sivachoerus* (Suidae, Artiodactyla) and *Hexaprotodon* (Hippopotamidae, Artiodactyla) (Sein and Thein 2013; Egi et al. 2018; Sein 2020; Takai et al. 2021; Longuet et al. 2023).

Materials and methods

The fossil specimens described were collected by villagers during farm work between 2017 and 2022 in the Tebingan area including several villages such as Tebingan, Inbingan, Alebo, and Sanmagyi, about 50 km southeast of Magway City, Myanmar (Figure 2). The specimens were found in Inbingan village. They are now stored at the Department of Archaeology in Yangon, Myanmar. The terminology used in the present study and the post-cranial measurement method follow Guérin (1980). The Myanmar specimens have been compared to several genera of Rhinocerotidae: *Pliorhinus*, *Lartetotherium*, *Plesiaceratherium*, and *Alicornops* from Eurasia; *Gaindatherium*, and *Prosantorhinus* from Pakistan; *Chilotherium* from China and Pakistan; *Aceratherium* from Thailand; *Acerorhinus* from China; and *Brachypotherium*, *Rhinoceros*, and *Dicerorhinus* found in Thailand, the Indian subcontinent, China, and Myanmar (Ringström 1924; Heissig 1972; Deng 2005; Jin and Liu 2009; Khan 2009; Tong and Guérin 2009; Antoine 2012; Antoine et al. 2013; Deng et al. 2013; Handa et al. 2021).

Ratio diagrams used in this study follow Pandolfi and Tagliacozzo (2015): $A = \log_{10}(a/b) = \log_{10}(a) - \log_{10}(b)$; A = difference in log value; a = measurement of studied specimen, and b = measurement of the standard specimen. Here, the standard specimen used is *Diceros bicornis* from Guérin (1980). Each average measurement of the standard specimen was selected for ratios. This method is used to compare the proportions between the studied and the standard specimen.

Institutional and anatomical abbreviations. NMMP-KU-IR, National Museum of Myanmar Palaeontology, Kyoto University, Irrawaddy. MNHN, Muséum national d'Histoire naturelle, Paris. Mc, metacarpal. Mt, metatarsal.

Systematic palaeontology

Order Perissodactyla Owen, 1848
Family Rhinocerotidae Gray, 1821
Subfamily Rhinocerotinae Gray, 1821
Tribe Rhinocerotini Gray, 1821
Subtribe Rhinocerotina Owen, 1845
Genus *Rhinoceros* Linnaeus, 1758
Rhinoceros sp.

Materials (Figures 3, 4 and Tables S1, S2)

NMMP-KU-IR-6144, right distal humerus; NMMP-KU-IR-6146, right proximal radius; NMMP-KU-IR-4418, right McIII; NMMP-KU-IR-4419, right McIV; NMMP-KU-IR-6141, left distal femur; NMMP-KU-IR-6529 and NMMP-KU-IR-5912, two left tibias; NMMP-KU-IR-4913, a right distal tibia; NMMP-KU-IR-6117, a left astragalus; and NMMP-KU-IR-6006, a left calcaneus.

Locality and age

Inbingan village, Tebingan area, Magway Region, central Myanmar, early Late Miocene.

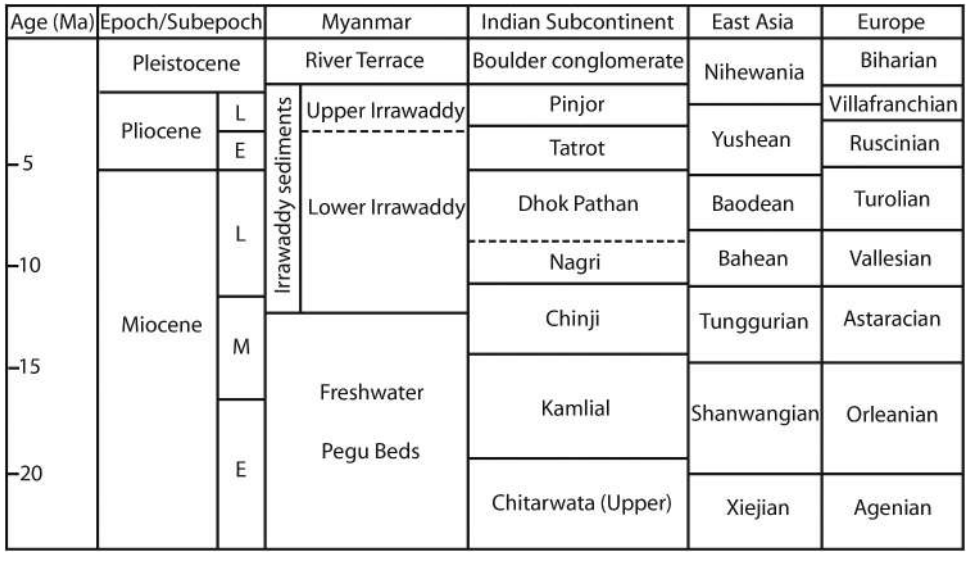

Figure 1. Stratigraphy of Neogene sediments in central Myanmar and correlations with stratigraphy of the Indian subcontinent, East Asia and Europe.

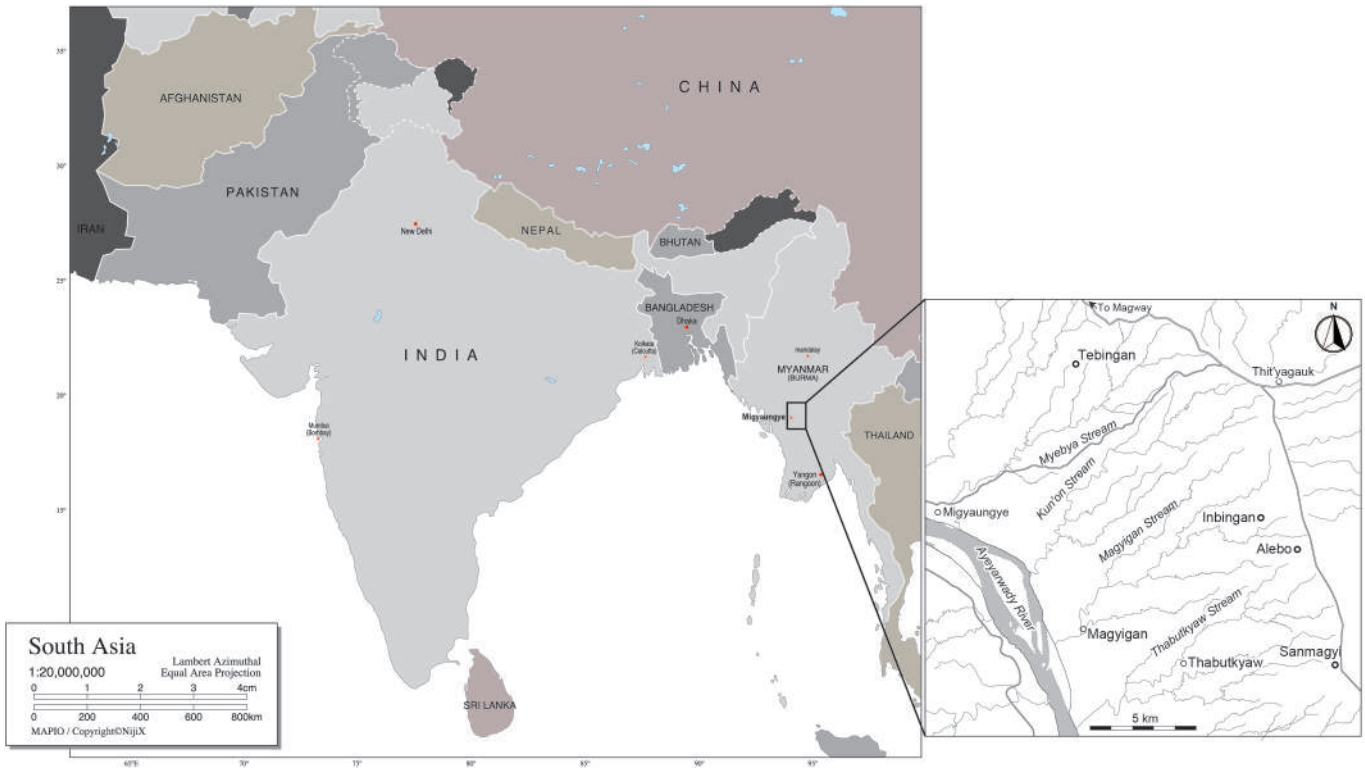

Figure 2. Index map of the Tebingan area, central Myanmar (modified after Longuet et al. 2023). Fossils are discovered from a wide range of Tebingan, Inbingan, Albo, and Sanmagyi villages.

Description

Humerus. In the anterior view, NMMP-KU-IR-6144 have a wide and deep trochlea, with the medial lip more voluminous than the lateral lip (Figure 3A). The coronoid fossa is deep, low, and wider than it is high. In the medial view, the trochlea is rounded. The diaphysis is thin and round. In the posterior view, the olecranon fossa is low and deep.

Radius. The coronoid process is elongated and pointed in NMMP-KU-IR-6146 (Figure 3(B-D)). The proximal articular surface is concave. In the medial view, the anterior face is flat, while the posterior face is concave. In the posterior view, the proximal ulnar facet is wide.

McIII. The facet for the magnum in NMMP-KU-IR-4418 is visible in the anterior view (Figure 3(E-G)). The facet for the unciform is oval. The diaphysis is flattened anteroposteriorly. In lateral view, the posterior facet of the McIV is missing; the anterior facet appears to be higher and oblique, and there is a large depression between the two facets. The insertion area for the extensor metacarpi radialis is flat. The diaphysis is oval but slightly pinched on the lateral side.

McIV. NMMP-KU-IR-4419 (Figure 3(H-J)) has an arched diaphysis. The proximal facet for the cuboid is slightly concave and oval, and it occupies the entire proximal surface. There is a notch on the posterior edge of the articular surface. The lateral surface does not have an articular surface; the bone is concave, with a more pronounced concavity in the distal part. The medial surface has two facets corresponding to the McIII. The anterior facet appears rounded, the posterior facet is slightly lower and smaller than the anterior facet. In the medial view, there is a small notch on the diaphysis located on the lower half, followed by a depression.

Femur. (Figure 4(A-B)). In the anterior view, the medial condyle is slightly larger than the lateral one NMMP-KU-IR-6141. In the posterior view, the intercondylar fossa is deep.

Tibia. In NMMP-KU-IR-6529 (Figure 4(C-F)), the proximal view shows that the tibial tuberosity is relatively small but projected outwards. The lateral side is shallow, and the ligament groove is moderately deep. The medial tuberosity is rounded. The central intercondylar eminence is wide and deep. In the anterior view, the lateral lip is higher and slightly longer than the mesial lip. The epiphyses are broad, while the diaphysis is thinner. In the lateral view, the articular surface for the fibula is wide but shallow across all three specimens. The posterior apophysis is rounded and low in NMMP-KU-IR-6529 (Figure 4(C-F)). For NMMP-KU-IR-5912 and NMMP-KU-IR-4913 (Figure 4(G-K)), the diaphysis is triangular with a sharp crest in the medial view and a broader, flatter part in the posterior view. In the anterior view, the distal part is wide Additionally, the posterior process is low and rounded in NMMP-KU-IR-5912 and NMMP-KU-IR-4913. NMMP-KU-IR-5912 is the largest (Table S2).

Astragalus. In the anterior view, the collum tali (neck between the trochlea and distal articulation) is high, and the groove of the trochlea is shallow in NMMP-KU-IR-6117 (Figure 4(L-O)). The facet for the fibula is flat. In the posterior view, the posterolateral facet for the calcaneus is round and concave. The medial and distal facets are not visible. In the distal view, the navicular facet is fairly wide and concave, and the angle with the facet for the cuboid is well-marked.

Calcaneus. In the anterior view, the apex of the calcaneus is broad in NMMP-KU-IR-6006, and the tuber is rather thin (Figure 4(P-Q)). In the medial view, the anterior border is concave, and the posterior

Figure 3. Forelimb bones of *Rhinoceros* sp. from Tebingan area, central Myanmar. (A) NMMP-KU-IR-6144, right distal humerus; (B-D) NMMP-KU-IR-6146, right proximal radius; (E-G) NMMP-KU-IR-4418, right McIII; and (H-J) NMMP-KU-IR-4419, right McIV. (A, B, E, and H) in anterior view; (C, F, and I) in posterior view; (G and J) in lateral view; and (D) in medial view. Scale bar = 10 mm.

border is slightly convex. There is also a significant difference between the height of the apex and the prominent anterior tuberosity. If the distal part of the calcaneus is broken, the angle between the main corpus of the calcaneus and the astragalus facets cannot be observed.

Comparisons and discussion

Due to the large number of specimens described, we have opted to limit comparisons. We focused on the three tibiae mentioned above, as they are the most abundant. However, the proportions of other specimens, including the humerus, radius, metacarpals III and IV, femur, astragalus, and calcaneus, are illustrated in the ratio diagrams (Fig. S1 and S2). The tibiae (NMMP-KU-IR-6529, NMMP-KU-IR-5912, and NMMP-KU-IR-4913) (Figure 4(C-K)) are close to the *Rhinoceros* genus in having a massive anterior tuberosity and outwardly inclined, on the tibial spine, the internal lip is lower than the external lip, with a deep central intercondylar eminence, a feature typical of Asian species (Guérin 1980). In addition, *Rhinoceros* has a low and rounded caudal apophysis and a shallow mediodistal gutter (Antoine 2002). Additionally, the proportions of NMMP-KU-IR-5912 are closer to those of *R. unicornis*, and the proportions of NMMP-KU-IR-6529 and NMMP-KU-IR-4913 are closer to those of *R. sondaicus*, suggesting that a large rhinoceros was present in the Tebingan area. They are different from *Brachypotherium* of Thailand, which has a higher posterior apophysis, a shallow central intercondylar eminence, and a shallow ligament groove (Handa et al. 2021). Furthermore, the proportions of the diaphysis of *Brachypotherium* are larger than those of NMMP-KU-IR-4913 and NMMP-KU-IR-6529 (Fig. S2). Cf. *Gaindatherium* from Israel has a distal articular surface that is wider than deep and less developed than the distal epiphysis (Pandolfi et al. 2021). The tibia of *Alicornops* has a triangular diaphysis with a strong lateral edge (Cerdeño and Sánchez 2000). Furthermore, the Myanmar specimen's ratios are, in general, larger than those of *Alicornops* (Fig. S2). In the proximal view, *Chilotherium* has a medial condyle larger than the lateral condyle

Figure 4. Hindlimb bones of *Rhinoceros* sp. from Tebingan area, central Myanmar. (A-B) NMMP-KU-IR-6141, left distal femur; (C-F) NMMP-KU-IR-6529, left tibia; (G-H) NMMP-KU-IR-5912, a left tibia; (I-K) NMMP-KU-IR-4913, right distal tibia; (L-O) NMMP-KU-IR-6117 left astragalus; and (p-Q) NMMP-KU-IR-6006, left calcaneus. (C, I, L, and P) in anterior view; (F) in proximal view; (D, G, J, and M) in posterior view; (E-,H, and N) in lateral view; (K and O) in distal view; and (Q) in medial view. Scale bar = 20 mm.

and the medial intercondyloid tubercle is wider than the lateral one, and both have the same length (Deng 2002). In addition, the three Myanmar specimens are larger than *Chilotherium* which the proportions are very low (Fig. S2). The three specimens from the Tebingan area also do not belong to the *Pliorhinus* because in this genus, the tibial tuberosity is rounded and thin, the tibial groove is shallow and wide, and the central intercondyloid is closed posteriorly and has a V-shape. The diaphysis is slightly narrower than its distal part (Pandolfi et al. 2021). The proportions of NMMP-KU-IR -6529 and NMMP-KU-IR-4913 are in general lower than those of *Pliorhinus* while NMMP-KU-IR-5912 has larger ratios than those of *Pliorhinus* (Fig. S2). Specimens from the Tebingan area do not belong to the *Aceratherium* which has an intercondylar eminence that is not prominent, and in the posterior view, the posterior apophysis is high and rounded (Hünerman 1989). Furthermore, the proportions of *Aceratherium* are lower than those of NMMP-KU-IR-6529, NMMP-KU-IR-5912, and NMMP-KU-IR-4913.

The specimens have therefore been assigned to the genus *Rhinoceros*. Within *Rhinoceros* species, the main differentiating feature between *R. unicornis* and *R. sondaicus* is the size of the elements. Indeed, the tibia of *R. unicornis* is longer than that of *R. sondaicus* (Guérin 1980; Antoine 2002); the trochlea of the humerus is wide and oblique in *R. unicornis*, and the olecranon fossa is narrow, low, and oval (Filoux and Suteethorn 2018). The calcaneus of *R. unicornis* is slightly more massive than that of *R. sondaicus*. The latter has a collum tali that is shaped like a deep hole, typical of *R. sondaicus* (Guérin 1980). The proportions of Tebingan specimens approach those of *Rhinoceros*. More specifically, the ratios of the humerus (NMMP-KU-IR-6144), femur (NMMP-KU-IR-6141), tibia (NMMP-KU-IR-6529), and astragalus (NMMP-KU-IR-6117) are close to those of *R. sondaicus* (Fig. S1 and S2). The proportions of the radius (NMMP-KU-IR-6146), tibia (NMMP-KU-IR-5912), and calcaneus (NMMP-KU-IR-6006) are closer to those of modern *R. unicornis* and the proportions of NMMP-KU-IR-6146 are like those of *R. unicornis* from Kanchanaburi, Thailand (Filoux and Suteethorn 2018) (Fig. S1). The combination of morphology and ratios makes it possible to assign specimens of the tibia specimen NMMP-KU-IR-5912 to a large *Rhinoceros* sp. The other specimens can be assigned to a smaller *Rhinoceros* sp.

Rhinoceros cf. *R. sondaicus*

Materials (Figure 5A-D and Table S2)

NMMP-KU-IR-5914, left astragalus.

Locality and age

Inbingan, Tebingan area, Magway Region, central Myanmar, early Late Miocene.

Description

Astragalus. The trochlea is wide and deep in NMMP-KU-IR-5914 (Figure 5(A-D)). In the anterior view, the collum tali is high and deep. The facet with the fibula is flat and oblique. In the posterior view, the posterior facet for the calcaneus is concave and diamond-shaped, and the extension of the facet is wide. The medial facet for the calcaneus is wide and nearly triangular. Distally, the facet joint is broken at the posterior edge. The distal articular surface is also wide and slightly concave.

Figure 5. Post-cranial remains of *Rhinoceros* cf. *R. sondaicus* (A-D) and *Dicerorhinus* sp. (E-G) from Tebingan area, central Myanmar. (A-D) NMMP-KU-IR-5914, left astragalus and (E-H) NMMP-KU-IR-4413, left calcaneus. (A and E) in the anterior view; (B) in the posterior view; (C and G) in the lateral view; and (D and F) in the medial view. Scale bar = 10 mm.

Comparisons and discussion

NMMP-KU-IR-5914 is remarkably similar to other *Rhinoceros* in having a deep, wide trochlea, a triangular medial facet, a low collum tali, the facet for the navicular and cuboid are separated by an obtuse ridge, and the whole articulation is wide with an oblique anterior edge in *Rhinoceros* (Guérin 1980; Antoine 2002). Compared with other Southeast Asian genera, NMMP-KU-IR -5914 does not belong to *Chilotherium*, which has a narrow trochlea, concave navicular facet, a long distal extension on the posterior facet and a small and oval medial facet (Heissig 1972). Furthermore, the proportions of *Chilotherium* are lower than those of NMMP-KU-IR-5914 (Figure 2S). NMMP-KU-IR-5914 do not belong to *Brachypotherium* which has a shallow and wide trochlea, a high collum tali, and an almost flat posterior facet for the calcaneus in lateral view (Handa et al. 2021). Furthermore, the proportions of the trochlea of the *Brachypotherium* astragalus are smaller than those of NMMP-KU-IR-5914, but the proportions of the distal part of the *Brachypotherium* astragalus are larger than those of NMMP-KU-IR-5914 (Fig. S2). The astragalus of *Aceratherium* has an oblique axis between the trochlea and the articular surface for the navicular. In addition, the collum tali is low and shallow (Hünerman 1989). NMMP-KU-IR-5914 cannot be assigned to *Lartetotherium*, because the trochlea is wide and the medial lip almost reaches the edge of the facet for the navicular, the posterior facet for the calcaneus is large with a short distal extension and the medial facet is oval (Cerdeño 1986). The proportions of *Lartetotherium* are larger than those of NMMP-KU-IR-5914 (Fig. S2). NMMP-KU-IR-5914 do not belong to *Dihoplus*, because the medial facet for the calcaneus of this genus is large and has an irregularly subcircular outline and is always in contact with the distal facet for the calcaneus. Furthermore, the lower border of the bowed articular stripe of the astragalus is smoothly concave and bears a small convex expansion in its middle (Giaourtsakis 2009). The trochlea of the *Pliorhinus* astragalus is wide and asymmetrical, the lateral lip is wide and globular and the facet of the fibula is vertical (Pandolfi et al. 2021), unlike NMMP-KU-IR-5914, which has an oblique facet for the fibula. Unlike NMMP-KU-IR -5914 (Heissig 1972), the astragalus of *Gaindatherium* has a medial facet always attached to the distal facet for the calcaneus, the medial facet for the calcaneus varies from nearly rectangular to sub-oval, and the collum tali is high but also not deep. Finally, in *Dicerorhinus*, the astragalus has a distinctly narrower trochlea than other species and the proportions of the astragalus of *Dicerorhinus* are smaller than those of NMMP-KU-IR-5914 (Guérin 1980).

NMMP-KU-IR-5914 is close to *Rhinoceros*. In total, five species of *Rhinoceros* can be considered valid: *R. platyrhinus* Falconer and Cautley, 1846; *R. sinensis* Owen, 1870; *R. sivalensis* Falconer and Cautley, 1847; *R. sondaicus* Desmarest, 1822; and *R. unicornis* Linnaeus, 1758. Unfortunately, *R. platyrhinus* and *R. sivalensis* have only been studied using cranial remains (Colbert 1938; Khan 2009; Pandolfi and Maiorino 2016). NMMP-KU-IR-5914 was therefore compared with the species *R. sinensis*, *R. sondaicus*, and *R. unicornis*, for which the astragalus has been studied (Guérin 1980; Antoine 2002; Jin and Liu 2009; Khan 2009). The astragalus of *R. unicornis* has larger proportions than NMMP-KU-IR-5914, the collum tali is shaped like a gutter, and the distal tubercle is well-developed. NMMP-KU-IR-5914 has characteristics typical of *R. sondaicus*. Indeed, this species is characterised by a very deep collum tali forming a hole (Guérin 1980). An astragalus belonging to *R. sondaicus* from Khok Sung also has a very deep collum tali, a facet for the navicular extends onto the anterior part of the astragalus (Suraprasit et al. 2016). The proportions of NMMP-KU-IR-5914 are closer from *R. sondaicus*. The astragalus of *R. sinensis* (Jin and Liu 2009) is narrower proximo-distally in the anterior view compared to NMMP-KU-IR-5914. The collum tali is low, and the

trochlea is shallow. In the posterior view, the posterior facet for the calcaneus is rather square-shaped, with a narrow facet extension (Jin and Liu 2009). The proportions of *R. sinensis* are smaller than those of NMMP-KU-IR-5914.

The characteristics that allow assignment of NMMP-KU-IR -5914 to *Rhinoceros* cf. *R. sondaicus* are the presence of wide and deep trochlea, a deep collum tali in the shape of a hole, and the proportions of the astragalus.

R. sondaicus is currently known from the early Pleistocene in the Indian subcontinent, South and Southeast Asia (Antoine 2012). Furthermore, *R. sondaicus* is already known from Myanmar, probably from the Plio-Pleistocene (Zin-Maung-Maung-Thein et al. 2010). The discovery of one astragalus assigned to cf. *R. sondaicus* from the Tebingan area displaying similar characteristics to *R. sondaicus* is based on post-cranial remains. To be certain of the presence of *R. sondaicus* during the early Late Miocene, other discoveries of cranial remains in the Tebingan area are needed.

Genus *Dicerorhinus* Gloger, 1841
Dicerorhinus sp.

Materials (Figure 5E-G and Table S2)
NMMP-KU-IR-4414, left calcaneus.

Locality and age
Inbingan village, Tebingan area, Magway Region, central Myanmar, early Late Miocene.

Description
Calcaneus. The tuber of NMMP-KU-IR-4414 (Figure 5(E-G)) is shorter than that NMMP-KU-IR-6006, which was identified as *Rhinoceros* sp. The top of the calcaneus is rounded, and the rostrum calcanei is prominent. In the anterior view, the facet for the fibula is present on the proximal facet for the astragalus. In the medial view, the anterior and posterior face of the tuber are concave. Additionally, the difference between the maximum apex and the anterior tuber in NMMP-KU-IR-4414 is smaller compared to NMMP-KU-IR-6006. The sustentaculum tali forms an obtuse angle with the tuber. Distally, the proximal facet of the astragalus is convex and rather round and the medial facet of the astragalus is slightly triangular. A shallow gutter separates the two facets. The distal facet for the astragalus is nearly rectangular and small. The facet for the cuboid is rectangular.

Comparisons and discussion
The calcaneus was compared with that of extant *Dicerorhinus* (MNHN-ZM-AC-A7967, MorphoSource 2013) and with the description of the calcaneus of *D. sumatrensis* from Guérin (1980). The Tebingan specimen can be assigned to *Dicerorhinus* based on the following characteristics in having a short tuber, the sustentaculum tali forms a obtuse angle with the tuber, and the difference between the apex and the anterior tuberosity is not large compared to *Rhinoceros*. The proportions of NMMP-KU-IR-4414 are, in general, slightly larger than those of *Dicerorhinus* (Fig. S2). NMMP-KU-IR -4414 does not belong to *Brachypotherium* because the calcaneal process is elongated, the distal articular surface is narrow, and the proximal facet for the astragalus does not have the facet for the fibula (Heissig 1972). Furthermore, the proportions (Height and transverse diameter sustentaculum tali) of the calcaneus of *Brachypotherium* are larger than those of NMMP-KU-IR-4414 (Fig. S2). NMMP-KU-IR -4414 does not belong to *Prosantorhinus* because the calcaneus of this genus has a short tuber with pronounced irregularities, a facet of the fibula is present, and a sustentaculum tali forms a right angle with the tuber (Cerdeño 1996). In *Aceratherium*, the articular surface for the cuboid is crescent-shaped, and the angle between the tuber and the sustentaculum tali forms a right angle (Hünerman 1989). Additionally, the proportions of the height of the *Aceratherium* calcaneus are lower than the height of NMMP-KU-IR-4414 (Fig. S2). NMMP-KU-IR-4414 cannot be assigned to *Alicornops* because the calcaneus of *Alicornops* is small, with a short and wide tuber, and the sustentaculum tali forms a right angle with the tuber (Cerdeño and Sánchez 2000) (Fig. S2). The calcaneus of *Lartetotherium* is different from NMMP-KU-IR-4414 in having a large tuber, the sustentaculum is inclined to the vertical axis, and regarding the proportions the total length and the width of the tuber of the calcaneus is greater than NMMP-KU-IR-4414 (Cerdeño 1986) (Fig. S2). The calcaneus of *Pliorhinus* has a transversely curved sustentaculum tali and a very massive tuberosity, with higher proportions compared to the Tebingan specimen (Pandolfi et al. 2021). Finally, the calcaneus of *Chilotherium* is relatively smaller than NMMP-KU-IR-4414 with a shorter tuber, the calcaneal process is weak, and the sustentaculum tali is very flat (Heissig 1972). NMMP-KU-IR-4414 is slightly wider than the known *Dicerorhinus*, but it can be assigned as *Dicerorhinus* sp.

Dicerorhinus has long been considered a wastebasket taxon. However, several authors recently assigned some *Dicerorhinus* species to *Stephanorhinus*, *Dihoplus*, and *Lartetotherium* (Antoine et al. 2003; Tong 2012; Li and Deng 2023). Therefore, *Dicerorhinus* comprises four species: *D. cixianensis* Chen and Wu 1976 from China; *D. fusuiensis* from China; *D. gwebinensis* Zin-Maung-Maung -Thein et al. 2008 from Gwebin, Myanmar; and the modern species *D. sumatrensis* Fisher 1814 from Sumatra. Initially, *D. fusuiensis* was described initially as *R. fusuiensis* by Yan et al. (2014) but was subsequently reassigned to *Dicerorhinus* by Antoine et al. (2022) through phylogenetic analyses. In addition, *D. cixianensis* was recently reassigned to the genus *Lartetotherium* by Li and Deng (2023) due to new comparisons between the skulls of *Dicerorhinus* and *Lartetotherium* cf. *L. sansaniense*. Now, the genus *Dicerorhinus* encompasses three species: *D. fusuiensis*, *D. gwebinensis*, and *D. sumatrensis*.

NMMP-KU-IR-4414 has been compared only to the modern species, *D. sumatrensis*. The other two *Dicerorhinus* species, *D. fusuiensis* from China (Yan et al. 2014, 2016), and *D. gwebinensis* from Myanmar (Zin-Maung-Maung-Thein et al. 2008) are known only from cranial remains. Yan et al. (2014, 2016) described *R. fusuiensis* using both cranial and post-cranial remains. *R. fusuiensis* has been reassigned to *D. fusuiensis* through phylogenetic analysis, showing that *R. fusuiensis* was close to *Dicerorhinus* (Antoine et al. 2022). Two species were found during the Plio-Pleistocene of central Myanmar: *Dicerorhinus gwebinensis*, described from a skull found in Gwebin area, central Myanmar dated from the Late Pliocene (4–2 Ma) (Zin-Maung-Maung-Thein et al. 2008) along with a mandible identified as *Dicerorhinus* cf. *D. sumatrensis* at Sulegone locality, Pauk Township (Zin-Maung-Maung-Thein et al. 2010). Based on cranio-dental proportions, *D. gwebinensis* appears to be slightly wider than the modern species *D. sumatrensis*. The calcaneus proportions presented in this study are also slightly wider than those of *D. sumatrensis*. These proportions, along with the discovery of both specimens in central Myanmar, might suggest that the calcaneus could possibly be closer to *D. gwebinensis*.

Figure 6. Metacarpals of *Brachypotherium perimense* from Tebingan area, central Myanmar. (A, D, and G) NMMP-KU-IR-5228, right McII; (B, E, and H) NMMP-KU-IR -5230, right McII, and (C, F, and I) NMMP-KU-IR-5227, right McIII. (A-C) in anterior view; (D-F) in posterior view; and (G-I) in lateral view. Scale bar = 10 mm.

Subtribe Teleoceratina Hay, 1902
Genus *Brachypotherium* Roger, 1904
Brachypotherium perimense Falconer and Cautley, 1847

Geographic and stratigraphic ranges
Southeast Asia, spanning the Miocene.

Materials (Figure 6 and Table S1)
NMMP-KU-IR-5228 and NMMP-KU-IR-5230, two right McII; NMMP-KU-IR-5227, right McIII.

Locality and age
Inbingan village, Tebingan area, Magway Region, central Myanmar, early Late Miocene.

Description
McII. NMMP-KU-IR-5228 (Figure 6(A, D, G)) and NMMP-KU-IR -5230 (Figure 6(B, E, H)) The facet for the trapezoid is very concave and saddle-shaped in the anterior view in NMMP-KU-IR-5228 (Figure 6(A, D, G) and NMMP-KU-IR-5230 (Figure 6(B, E, H)). In the posterior view, the trapezoid facet on the medial side is small. In the lateral view, the facet with the McIII and the magnum is reniform, and the junction between these two facets is slightly visible on the left, but the facet for the McIII is not visible in NMMP-KU-IR-5230. The facets are more laterally oriented in NMMP-KU-IR-5230 than in NMMP-KU-IR-5228, where they appear more posteriorly oriented. The diaphysis in both specimens is elliptical.

McIII. The bone is flat anteroposteriorly. In the anterior view, the facet for the magnum is not visible in NMMP-KU-IR-5227 (Figure 6(C, F, I)). The unciform is flat, and small compared to the facet for the magnum. There are two spaced facets, one responding to the unciform and located close to the facet for magnum, and one posterior facet. The posterior facet is wide and trapezoidal, and the second facet for McIV is more rounded. There is a depression between these two facets. The insertion zone of the extensor metacarpi radialis is flat (anterior zone, proximal part of the bone). The section of the bone is oval/flattened. The distal epiphysis is wider than the proximal one.

Comparisons and discussion
NMMP-KU-IR-5228, NMMP-KU-IR-5230, and NMMP-KU-IR -5227 can be assigned to *Brachypotherium* in having the posterior facet for the McIII always absent on the McII, the facet for the magnum is kidney-shaped and always visible in the anterior view (Antoine 2002) (Figure 7(K-L)). The specimens cannot be assigned to *Dicerorhinus* because the McII has a very prominent upper tuberosity and the diaphysis is triangular (Guérin 1980), and the proportions of the McII are lower compared to the Tebingan specimens (Fig. S1). The proportions of the Tebingan specimens are close to those of *Rhinoceros*, but morphologically different. Indeed, in *Rhinoceros*, the posterior facet for McIII is always present on the McII (character 226, Antoine 2002), and the facet for magnum is always visible on the McIII in the anterior view (character 229, Antoine 2002) (Figure 7(A-D)), these features are not observable in NMMP-KU-IR-5228, NMMP-KU-IR-5230, and NMMP-KU-IR -5227. In *Aceratherium*, the metapodials are robust, with a large diaphysis; on the McIII, the facet for the magnum is visible on the

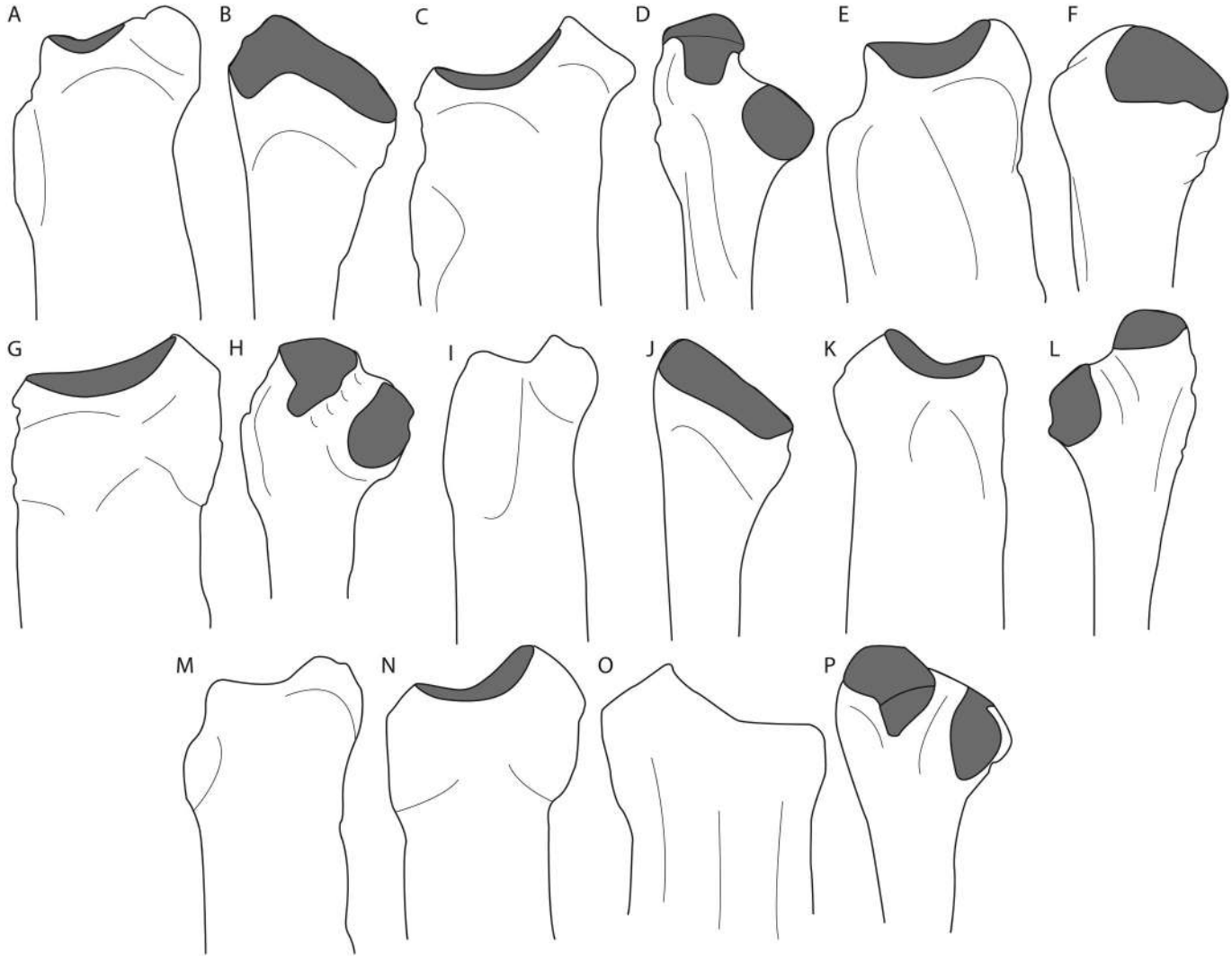

Figure 7. McII (A-B, E-F, I-J, and M) and McIII (C-D, G-H, K-L, and N-P) of selected compared specimens (A-B) McII and (C-D) McIII of *Rhinoceros unicornis* from the late Pleistocene of western Thailand (Filoux and Suteethorn 2018); (E-F) McII and (G-H) McIII of *Aceratherium incisivum* from the Pliocene of Höwenegg (Germany) (Hünerman 1989); (I-J) McII and (K-L) McIII of *Pliorhinus miguelcrusafonti* from Plio-Pleistocene of Georgia (Pandolfi et al. 2021); (M) McII of *chilotherium wimani* from the Late Miocene of China (Deng 2002); (N-P) McII and McIII of *Brachypotherium perimense* from the Middle Siwalik of Pakistan (Heissig 1972).In anterior view (A, C, E, G, I, K, and M-O) and lateral view (B, D, F, H, J, L, and P).

anterior view; and, on the McII, the facet for the trapezoid is shallow (Hünerman 1989) (Figure 7(E-H)). The proportions of Myanmar specimens are larger than those of *Aceratherium* (Fig. S1). The diaphysis of the McII and McIII of *Alicornops* is almost as wide as the distal epiphysis, the facet for the magnum is almost flat on the McIII (Cerdeño and Sánchez 2000), and the proportions of *Alicornops* are lower than those of the Tebingan specimens (Fig. S1). NMMP-KU-IR-5228, NMMP-KU-IR-5230, and NMMP-KU-IR-5227 cannot be assigned to *Pliorhinus* because the McII is long and graceful, the articular surface for the McIII is small, short, and appears straighter than the Tebingan specimens (Pandolfi et al. 2021). Furthermore, the proportions of the Myanmar specimens (height and transverse diameter diaphysis) are larger than those of *Pliorhinus* (Fig. S1). Nor can they be assigned to *Plesiaceratherium* from China, which has narrow metacarpals, and a facet of the magnum is visible in the anterior view of the McIII (Defa and Heissig 1986; Antoine 2002). Furthermore, the metacarpals proportions of *Plesiaceratherium* are lower than those of Myanmar specimens (Fig. S1). In *Gaindatherium*, the facet for the trapezoid is narrow and concave transversely, and the facet for the McIII is triangular (Heissig 1972). These comparisons show that NMMP-KU-IR-5228, NMMP-KU-IR-5230, and NMMP-KU-IR-5227 are closer to the *Brachypotherium*.

Brachypotherium embraces the Asian species *B. perimense*, '*B*'. *fatehjangense*, and *B. gajense* (Pilgrim 1912; Antoine et al. 2013). *B. gajense* was originally described with dental remains by Pilgrim (1912) as *Aceratherium gajense*. Recent studies have shown its reassignment to *Brachypotherium* (Métais et al. 2009; Antoine et al. 2010). This species has mainly been found in the Chitarwata Formation from the early Miocene from the Bugti Hills (Métais et al. 2009; Antoine et al. 2010). The Tebingan specimens were therefore compared with the two Asian species most studied in the deposits: *B. perimense* and '*B*'. *fatehjangense* (Khan et al. 2010; Iqbal et al. 2013; Rafeh et al. 2020; Handa et al. 2021). The classification of '*B*". *fatehjangense* remains uncertain. Some researchers have placed it in different genera, such as *Aprotodon fatehjangense*, *Chilotherium* (as *C. fatehjangense* and *C. blanfordi*), or *Diaceratherium* (Heissig 1972, 1975; Deng 2006; Saña 2008). Saña (2008) suggested that "*B*". *fatehjangense* might be more closely related to *Diaceratherium* than to *Brachypotherium* and renamed it *D. fatehjangense*. However, this reclassification is based solely on phylogenetic analysis, with no detailed morphological descriptions

yet provided. Despite this, some recent publications still assign it to *Brachypotherium* (Rafeh et al. 2020; Handa et al. 2021; Samiullah et al. 2021), so we continue to refer it as "*B*'. *fatehjangense*, using quotation marks to indicate the ongoing debate.

Brachypotherium also includes two European species, *B. brachypus* and *B. goldfussi* and four African species, *B. heinzelini*, *B. snowi*, B. *lewisi*, and *B. minor* (Hooijer 1963; Hooijer and Patterson 1972; Geraads and Miller 2013; Koufos and Kostopoulos 2013). The Tebingan specimens are different from the African and European species. Indeed, the McII of *B. heinzelini* is relatively short (Hooijer 1966). Regarding *B. brachypus*, the facet for the trapeze on the McII is poorly developed and the lateral articulation of the McIII and the magnum is to be divided into two (Cerdeño 1993). Compared with Asian species, the McII of '*B*'. *fatehjangense* has a narrow facet for the trapezoid but deep like a saddle, a low and small facet of the trapeze, a reniform facet for the magnum, and there is no posterior facet for the McIII (Hooijer and Patterson 1972). The Tebingan specimens are close to *B. perimense*. On McII, the facet for the trapezium is present in the dorsal view; on the McIII, the facet for the magnum is concave and not visible on the anterior part; the facet for the unciform is curved around that of the magnum and is inclined laterally, and the McII facet is small (Heissig 1972) (Figure 7(K-L)). NMMP-KU-IR-5228, NMMP-KU-IR-5230, and NMMP-KU-IR-5227 can be assigned to *B. perimense* due to their similar morphology and proportions. The post-cranial bones of *B. perimense* studied here could thus be associated with the dental remains found in the Tebingan area (Longuet et al. 2023).

Rhinocerotidae indet.

Materials (Figure 8 and tables S1, S2)

NMMP-KU-IR-5091, 5910, and 6143, three left distal humeri; NMMP-KU-IR-5361, left proximal radius; NMMP-KU-IR-6008, right distal femur; NMMP-KU-IR-4413, right astragalus; and NMMP-KU-IR-4415, left calcaneus.

Locality and age

Inbingan village, Tebingan area, Magway Region, central Myanmar, early Late Miocene.

Description

Humerus. In the anterior view, the coronoid fossa is oval and deep in NMMP-KU-IR-5091, NMMP-KU-IR-5910, and NMMP-KU-IR-6143 (Figure 8(A-F)). The trochlea is wide and deep, with the

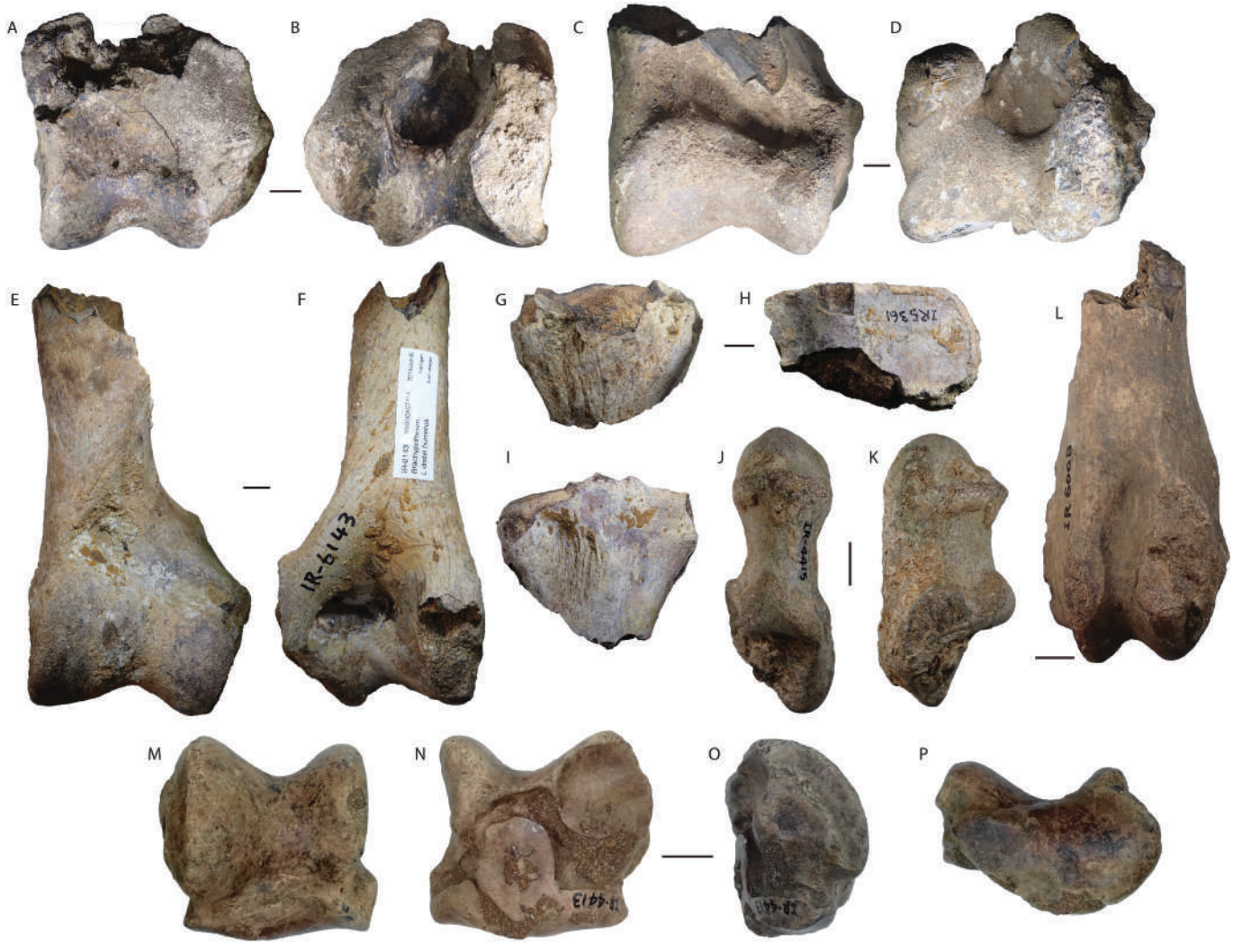

Figure 8. Limb bones of Rhinocerotidae gen. et sp. indet. From the Tebingan area, central Myanmar. (A-B) NMMP-KU-IR-5091; (C-D) NMMP-KU-IR-5910; (E-F) NMMP-KU-IR-6143; (G-I) NMMP-KU-IR-5361; (J-K) NMMP-KU-IR-4415; (L) NMMP-KU-IR-6008; and (M-P) NMMP-KU-IR-4414. (A, C, E, G, J, L, and M) anterior view; (B, D, F, I, and N) in the posterior view; (H) in the proximal view; (K) in the medial view; (O) in the lateral view; and (P) in the distal view. Scale bar = 20 mm.

medial (= trochlear) lip more developed than the lateral (= condylar) lip, and they are parallel. In the posterior view, the olecranon fossa is low and deep in all three specimens but rather round in NMMP-KU-IR-5091 and slightly oval in NMMP-KU-IR-6143. Additionally, the lateral edge of the epiphysis of NMMP-KU-IR -5910 is oblique.

Radius. In the proximal view, the two articular facets are still visible in NMMP-KU-IR-5361 (Figure 8(G-I)). The medial facet appears larger than the lateral facet. In the cranial view, the anterior edge of the proximal part is straight.

Femur. NMMP-KU-IR-6008 is a very poorly preserved right distal part of the femur, with only the trochlea of the femur preserved (Figure 8L). The bone is broken below the third trochanter, and the medial and lateral condyles are missing.

Astragalus. In the anterior view, the trochlea is deep, the collum tali is low and shallow, and the facet with the fibula is oblique and flat in NMMP-KU-IR-4413 (Figure 8(M-P)). In the posterior view, the posterior facet of the calcaneus is concave and rather rounded, and the extension of this facet is small and almost perpendicular. The distal facet of the calcaneus is elongated and connects to the medial facet of the calcaneus. The medial facet is slightly oval with a widening towards the medial side. Distally, the ulna-navicular facet is wide along the anteroposterior axis. The navicular facet extends onto the anterior part of the astragalus.

Calcaneus. In the medial view, the anterior part of NMMP-KU-IR -4415 is slightly concave, with a well-marked rostrum calcanei (Figure 8(J-K)). There is also a significant difference between the top of the calcaneus and the anterior tuber. The posterior part is straight. The impression of the sustentaculum tali shows that the angle between it and the tuber of the calcaneus appears rather acute. The proximal facet for the astragalus is convex, and the distal facet for the astragalus is small and elongated, leading to the facet for the cuboid.

Comparisons and discussion

Given the large number of specimens, only some have been compared. Since the number of humerus specimens is larger, three of them will be compared first. The humeri NMMP-KU-IR-5091, NMMP-KU-IR-5910, and NMMP-KU-IR-6143 differ from *Dicerorhinus* having a triangular-shaped and narrow olecranon fossa (Guérin 1980), and the proportions are lower compared to those of Tebingan specimens. The olecranon fossa is triangular in *Chilotherium* with lower proportions compared to the Tebingan specimens (Deng 2002). NMMP-KU-IR-5091, NMMP-KU-IR -5910, and NMMP-KU-IR-6143 are different from *Rhinoceros* which have a deep, low, and proximodistally elongated oval coronoid fossa (Guérin 1980; Antoine 2002). NMMP-KU-IR-5091, NMMP-KU-IR-5910, and NMMP-KU-IR-6143 are different from cf. *Gaindatherium* from Israel (Pandolfi et al. 2021). The coronoid fossa is deep, the olecranon fossa is wider than it is higher, and the lateral lips are straight (Pandolfi et al. 2021). Furthermore, the proportions of the distal part of Tebingan specimens are lower than those of cf. *Gaindatherium* (Fig. S1). As for *Alicornops*, this genus features a relatively small humerus with a large and deep olecranian fossa (Cerdeño and Sánchez 2000). In *Aceratherium*, the coronoid fossa is relatively narrow, the olecranon fossa is narrow and round, and the proportions are lower than those of the Tebingan specimens (Hünerman 1989) (Fig. S1). The Tebingan specimens differ from *Acerorhinus* which has a small, round coronoid fossa and a large, round olecranon fossa (Lu et al. 2021). *Pliorhinus* has a deep, triangular-shaped olecranon fossa that is wider than it is higher, a more developed medial lip than the lateral lip, and the trochlea is wider (Pandolfi et al. 2021). These features are similar to those of specimen NMMP-KU-IR-5910 (Figure 8(C-D)), but the proportions of the Myanmar specimen are smaller than those of *Pliorhinus* (Fig. S1). In Teleoceratina, such as *Prosantorhinus* and *Brachypotherium*, the long bones are wide and rather short, with epiphyses wider than the diaphysis (Cerdeño 1996). Most of the specimens present in this section are too fragmentary to be properly identified, and it is therefore preferable to assign them to Rhinocerotidae indeterminate.

Discussion

Previous work on dental remains of the Tebingan rhinoceroses

Rhinoceros sp. and *B. perimense* have already been identified by dental remains, indicating that *Rhinoceros* was distributed in central Myanmar since the early Late Miocene, probably arriving from the Indian subcontinent before the Late Miocene (Longuet et al. 2023). This migration was possible due to environmental changes in Myanmar, such as the retreat of the coastline to the south of Myanmar, giving way to a humid environment favorable to Rhinocerotidae (Zin-Maung-Maung-Thein et al. 2011; Habinger et al. 2022). *Brachypotherium* is a Miocene genus that lived in forest or wooded habitats, and possibly in semi-aquatic environments (Handa et al. 2018). Although no post-cranial remains belonging to *Brachypotherium* species have yet been found in Myanmar, newly discovered metacarpals of *B. perimense* confirm the presence of the species in central Myanmar during the early Late Miocene.

This archaic genus began to decline and gave way to modern genera such as *Rhinoceros* and *Dicerorhinus* during the late Miocene and disappeared at the Miocene-Pliocene boundary, possibly due to climatic causes (more arid climate) (Barry et al. 2002; Deng 2002).

New fossil records in Southeast Asia

Rhinoceros cf. *R. sondaicus* has been identified by an astragalus with similar characteristics to *R. sondaicus*: wide and deep trochlea and a very deep and low collum tali (Guérin 1980). In addition, the ratios of NMMP-KU-IR-5914 are closer to those of *R. sondaicus*. *R. sondaicus* has been known since the early Pleistocene in the Indian subcontinent, Thailand, Cambodia, Vietnam, and Sundaic region (Java, Malaysia, and Borneo), but fossil remains of this species are rare (Antoine 2012; Suraprasit et al. 2016). The oldest fossil records of *R. sondaicus* are dated to the Plio-Pleistocene of the Irrawaddy Formation, central Myanmar, through dental remains (Zin-Maung-Maung-Thein et al. 2010), thus suggesting a continental Asian origin of the species. It then migrated to the Southeast Asian islands during the Late Pleistocene (Zin-Maung-Maung-Thein et al. 2006). Nevertheless, fossil remains of *R. sondaicus* are rare during the Pleistocene in Southeast Asia (Antoine 2012). The recent discovery of an astragalus assigned to cf. *R. sondaicus* from the Tebingan area suggests a possible presence of *R. sondaicus* during the early Late Miocene of Myanmar and thus pushes back the occurrence of this species much earlier than previously thought. This supports a continental origin for the species. To confirm the presence of *R. sondaicus* in the Tebingan area, additional remains are necessary.

The genera *Rhinoceros* and *Dicerorhinus* are often found together in deposits. In the Early Pleistocene, *D. gwebinensis* Zin-Maung-Maung et al. 2008 and *Rhinoceros* sp. are found in the Gwebin area, Myanmar; *R. unicornis* and *D. sumatrensis* during the middle Pleistocene of Thailand, and the three modern species, *R. unicornis*, *R. sondaicus*, and *D. sumatrensis*, are found together

during the Late Pleistocene in different deposits in Vietnam and Sibrambang (Zin-Maung-Maung-Thein et al. 2008; Antoine 2012). Once again, *Rhinoceros* and *Dicerorhinus* were found together in the same early Late Miocene deposit in the Tebingan area, central Myanmar, as indicated by the identification of *Rhinoceros* cf. *R. sondaicus* and *Dicerorhinus* sp.

The genus *Dicerorhinus* is a rhinoceros with a frontal horn and a slender body compared to other Rhinocerotina. It lives preferentially in forests and near water (Groves and Kurt 1972). This genus has been known since the Pliocene in Myanmar with *D. gwebinensis* Zin-Maung-Maung-Thein et al. 2008, and since the Early Pleistocene in southern China, Thailand, Vietnam, Cambodia, Malaysia, Indonesia, Sumatra, and Borneo (Tong and Guérin 2009; Antoine 2012; Tong 2012; Yan et al. 2014, 2016) (Figures 9 and 10). The oldest representative of the genus *Dicerorhinus* is dated to the mid-Miocene and was described by Heissig (1972) in Pakistan under a species called *Didermocerus* aff. *sumatrensis*. The specimen is a second upper premolar (P2), from the Siwalik Chinji Formation in Siwalik described by Heissig (1972) (M 1956 II 268 - Tf. 5, Figs 1,2) is the only specimen assigned to *D. sumatrensis* from Pakistan. This specimen has a short crista and crochet and constricted protocone, whereas *D. sumatrensis* typically lacks crista and crochet on P2, and the presence of a constricted protocone is rather rare on P2 (Guérin 1980). Unfortunately, the material described is too poor to fully support this discovery. For some time, *Dicerorhinus* comprised four species: *D. gwebinensis*, *D. fusuiensis*, *D. sumatrensis*, and *D. cixianensis* (Zin-Maung-Maung-Thein et al. 2008, 2010; Tong and Guérin 2009; Tong 2012; Yan et al. 2014, 2016). *D. cixianensis* is known from the Mid-middle Miocene of China (Hebei province), which led to the hypothesis that *Dicerorhinus* descended into southeast Asia from the east. However, this hypothesis was refuted by the reassignment of *D. cixianensis* to the genus *Latertotherium* by Li and Deng (2023). *Dicerorhinus* is now known only from southeast Asia.

At the moment, the current discovery of post-cranial fossils of *Dicerorhinus* sp. from the early Late Miocene Tebingan fauna in central Myanmar represents the oldest fossil record of *Dicerorhinus* in Southeast Asia (Figure 10). *Dicerorhinus* may have originated in Southeast of Asia during the early Late Miocene and then migrated to the islands of Southeast Asia during the Pleistocene (Figure 9). This hypothesis is based on the identification of a calcaneus. It needs further support through the identification of cranial remains of *Dicerorhinus* in the Tebingan Area, central Myanmar. Furthermore, due to the dubious nature of the material referring to *Dicerorhinus* in Pakistan, the hypothesis of the genus's presence in Pakistan is

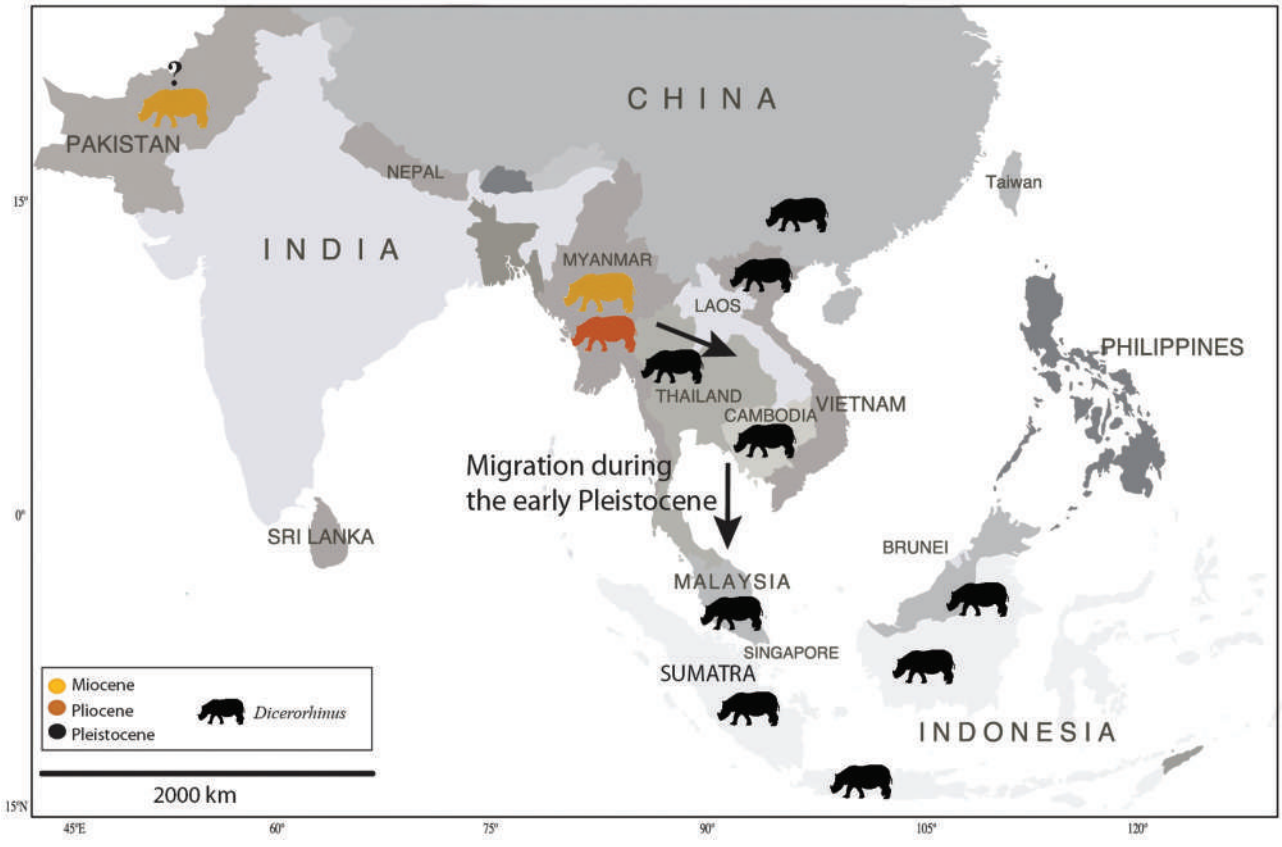

Figure 9. Geographical distribution of *Dicerorhinus* sp. in South and Southeast Asia during the Neogene and Pleistocene. Based on Tong and Guérin (2009) and Antoine (2012).

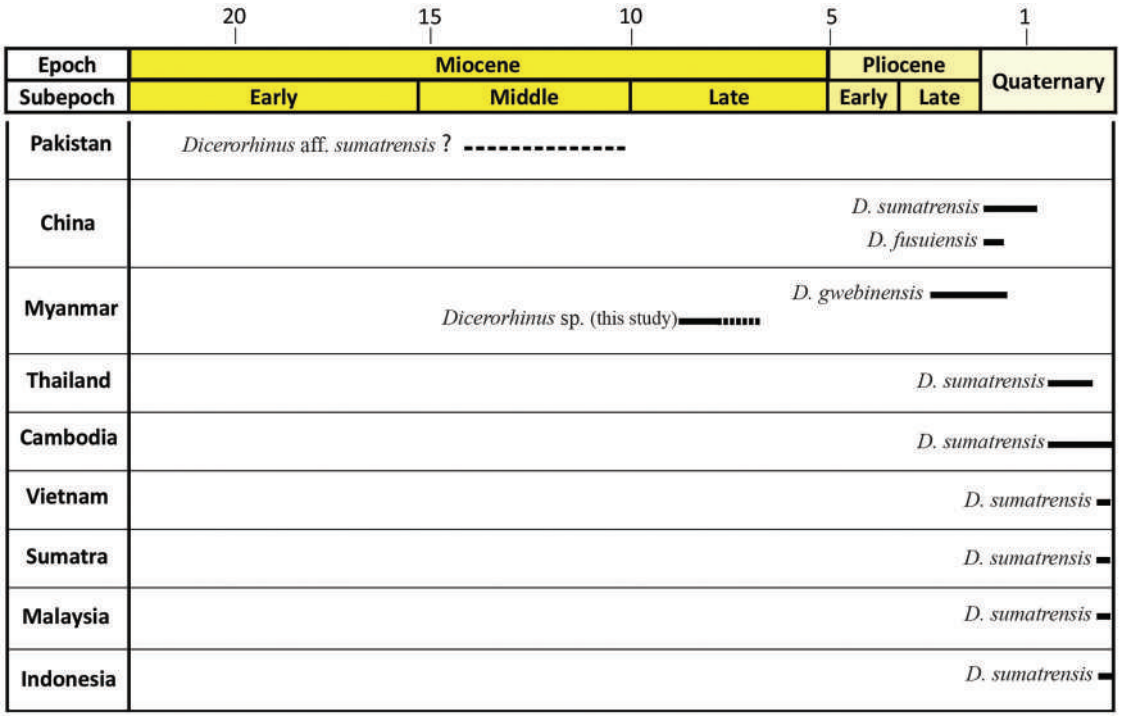

Figure 10. Chronology of *Dicerorhinus* sp. in South and Southeast Asia. Fossil record and locality according to Tong and Guérin (2009) and Antoine (2012).

not considered here. It would be interesting to know whether other material from Pakistan can be assigned to *Dicerorhinus* and thus confirm or not the hypothesis put forward in this paper.

Conclusion

The rhinoceros fossils from the lowermost part of the Irrawaddy Formation at the Tebingan include five taxa: *Rhinoceros* sp., *Rhinoceros* cf. *R. sondaicus*, *Dicerorhinus* sp., *B. perimense*, and Rhinocerotidae gen. et sp. indet. The presence of *Dicerorhinus* in the Tebingan area represents the oldest fossil record of the genus in Southeast Asia, indicating a continental Asian origin of this genus. Genera such as *Brachypotherium* likely began to decline at the end of the Miocene due to the fragmentation of forests, replaced by modern species of rhinoceros, such as *Rhinoceros* and *Dicerorhinus*.

The discovery of *Dicerorhinus* from the early Late Miocene (9–8 Ma) Tebingan fauna suggests the origin of the genus in Southeast Asia and then, it migrated to the islands of Southeast Asia during the Pleistocene. The retreat of the coastline southward in central Myanmar gave way to new terrestrial environments, such as forests and woodlands, thus favouring the arrival of *Dicerorhinus* and *Rhinoceros* during that period. Further detailed analysis of the complete dental remains of *Dicerorhinus* and *R. sondaicus* may confirm the presence of these species in the Tebingan area.

Acknowledgments

We gratefully thank the personnel of the Ministry of Education and the Ministry of Culture of the Union of Myanmar for granting our permissions for fieldwork in Myanmar. We also thank all members of the Myanmar-Japan joint Palaeontological Research Team and the curators of the National Museum of Myanmar for their assistance, and for providing us with access to their specimens. We would like to thank Drs. Nao Kusuhashi for providing the geological data of the study area. We would also like to thank the anonymous reviewers for their comments, which helped to improve this paper. This study was supported by JSPS KAKENHI (No. 22H02708 to M. Takai and No. JP22KK0048 to S. Tomiya), and by the Yamada Science Foundation (No. 1071 to M. Takai).

Disclosure statement

No potential conflict of interest was reported by the author(s).

Funding

The work was supported by the Japan Society for the Promotion of Science JSPS KAKENHI (No. 22H02708 to M. Takai and No. JP22KK0048 to S. Tomiya), and by the Yamada Science Foundation (No. 1071 to M. Takai).

ORCID

Morgane Longuet http://orcid.org/0000-0001-9422-2314

References

Antoine PO. 2002. Phylogénie et évolution des Elasmotheriina (Mammalia, Rhinocerotidae). Mem Mus Nat Hist Nat Paris. 188:1–359.

Antoine PO. 2012. Pleistocene and Holocene rhinocerotids (Mammalia, Perissodactyla) from the Indochinese Peninsula. Comptes Rendus Palevol. 11(2–3):159–168. doi: 10.1016/j.crpv.2011.03.002.

Antoine PO, Downing KF, Crochet JY, Duranthon F, Flynn LJ, Marivaux L, Métais G, Rajpar AR, Roohi G. 2010. A revision of *Aceratherium blanfordi* Lydekker, 1884 (Mammalia: Rhinocerotidae) from the Early Miocene of Pakistan: postcranials as a key. Zool J Linn Soc. 160(1):139–194. doi: 10.1111/j.1096-3642.2009.00597.x.

Antoine PO, Ducrocq S, Marivaux L, Chaimanee Y. 2003. Early rhinocerotids (Mammalia: Perissodactyla) from South Asia and a review of the Holarctic Paleogene rhinocerotid record. Can J Earth Sci. 40(3):365–374. doi: 10.1139/e02-101.

Antoine PO, Métais G, Orliac MJ, Rochet JY, Flynn LJ, Marivaux L, Rajpar AR, Roohi G, Welcomme JL. 2013. Mammalian Neogene biostratigraphy of the Sulaiman province, Pakistan. In: Wang X, Flynn LJ, Fortelius, editors. Fossil mammals of Asia. (NY): Columbia University Press; p. 400–422.

Antoine PO, Reyes MC, Amano N, Bautista AP, Chang CH, Claude J, De Vos J, Ingicco T. 2022. A new rhinoceros clade from the Pleistocene of Asia sheds light on mammal dispersals to the Philippines. Zool J Linn Soc. 194 (2):416–430. doi: 10.1093/zoolinnean/zlab009.
Barry JC, Morgan ME, Flynn LJ, Pilbeam D, Behrensmeyer AK, Raza SM, Khan AI, Badgley C, Hicks J, Kelley J. 2002. Faunal and environmental change in the late Miocene Siwaliks of northern Pakistan. Paleobiol. 28 (S2):1–71. doi: 10.1666/0094-8373(2002)28[1:FAECIT]2.0.CO;2.
Bender F. 1983. Geology of Burma. Berlin: Gebruder Bortraeger.
Cerdeño E. 1986. El esqueleto postcraneal de *Lartetotherium sansaniensis* (Mammalia, Rhinocerotadidae). Estud geol. 42:197–209. doi: 10.3989/egeol.86422-3748.
Cerdeño E. 1993. Étude sur *Diaceratherium aurelianense* et *Brachypotherium brachypus* (Rhinocerotidae, Mammalia) du Miocene moyen de France. Bull Mus Nat Hist Nat. 4:25–77.
Cerdeño E. 1996. *Prosantorhinus*, the small teleoceratine rhinocerotid from the Miocene of Western Europe. Geobios. 29(1):111–124. doi: 10.1016/S0016-6995(96)80077-5.
Cerdeño E, Sánchez B. 2000. Intraspecific variation and evolutionary trends of *Alicornops simorrense* (Rhinocerotidae) in Spain. Zool Scr. 29(4):275–305. doi: 10.1046/j.1463-6409.2000.00047.x.
Cerling TE, Harris JM, MacFadden BJ, Leakey MG, Quade J, Eisenmann V, Ehleringer JR. 1997. Global vegetation change through the Miocene/Pliocene boundary. Nature. 389(6647):153–158. doi: 10.1038/38229.
Chavasseau O, Chaimanee Y, Thura Tun S, Naing Soe A, Barry JC, Marandat B, Sudre J, Marivaux L, Ducrocq S, Jaeger JJ. 2006. Chaungtha, a new Middle Miocene mammal locality from the Irrawaddy Formation, Myanmar. J Asian Earth Sci. 28(4–6):354–362. doi: 10.1016/j.jseaes.2005.10.012.
Chen GF, Wu WY. 1976. Miocene mammalian fossils of Jiulongkou, Cixian district, Hubei. Vert PalAsiat. 14:8–10 (in Chinese with English summary.
Colbert EH. 1938. Fossil mammals from Burma in the American Museum of Natural History. Bull Am Mus Nat Hist. 75:255–436.
Colbert EH. 1943. Pleistocene vertebrates collected in Burma by the American Southeast Asiatic expedition. Am Philos Soc. 32:395–429, Plate 19–32.
Defa Y, Heissig K. 1986. Revision and Autopodial Morphology of the Chinese-European Rhinocerotid Genus *Plesiaceratherium* Young 1937. Zitteliana. 14:81–109.
Deng T. 2002. Evolution of Chinese Neogene Rhinocerotidae and its response to climatic variations. Acta Geol Sin. 76(2):139–145. doi: 10.1111/j.1755-6724.2002.tb00080.x.
Deng T. 2005. New discovery of *Iranotherium morgani* (Perissodactyla, Rhinocerotidae) from the late Miocene of the Linxia Basin in Gansu, China, and its sexual dimorphism. J Vertebr Paleontol. 25(2):442–450. doi: 10.1671/0272-4634(2005)025[0442:NDOIMP]2.0.CO;2.
Deng T. 2006. A primitive species of *Chilotherium* (Perissodactyla, Rhinocerotidae) from the late Miocene of the Linxia basin (Gansu, China). Cainozoic Res. 5:93–102.
Deng T, Hanta R, Jintasakul P. 2013. A new species of *Aceratherium* (Rhinocerotidae, Perissodactyla) from the late Miocene of Nakhon Ratchasima, northeastern Thailand. J Vertebr Paleontol. 33(4):977–985. doi: 10.1080/02724634.2013.748058.
Egi N, Ogino S, Takai M. 2018. Neogene Irrawaddy fauna of central Myanmar: Carnivora. Fossils. 104:21–33. (in Japanese with English abstract.
Filoux A, Suteethorn V. 2018. A late Pleistocene skeleton of *Rhinoceros unicornis* (Mammalia, Rhinocerotidae) from western part of Thailand (Kanchanaburi Province). Geobios. 51(1):31–49. doi: 10.1016/j.geobios.2017.12.003.
Geraads D. 2010. Rhinocerotidae. In: Werdelin L, Sanders DJ, editors. Cenozoic mammal of Africa. Berkeley: University of California Press; p. 669–683.
Geraads D, Cerdeño E, García Fernandez D, Pandolfi L, Billia E, Athanassiou A, Albayrak E, Codrea V, Obada T, Deng T, et al. 2021. A database of Old World Neogene and Quaternary rhino-bearing localities. www.rhinoresourcecenter.com/about/fossil-rhino-database.php.
Geraads D, Miller E. 2013. *Brachypotherium minor* n. sp. and other Rhinocerotidae from the Early Miocene of Buluk, Northern Kenya. Geodiversitas. 35(2):359–375. doi: 10.5252/g2013n2a5.
Giaourtsakis IX. 2009. The Late Miocene Mammal Faunas of the Mytilinii Basin. In: Rhinocerotidae. Beitr. Paläontol Vol. 31, Samos Island, Greece: New Collection; p. 157–187.
Groves CP, Kurt F. 1972. *Dicerorhinus sumatrensis*. Mamm Species. 21(21):1–6. doi: 10.2307/3503818.
Groves CP, Leslie DM. 2011. *Rhinoceros sondaicus* (Perissodactyla: Rhinocerotidae). Mamm Species. 43(887):190–208. doi: 10.1644/887.1.
Guérin C. 1980. Les rhinoceros (Mammalia, Perissodactyla) du Miocène terminal au Pleistocène Supérieur en Europe occidentale: comparaison avec les espèces actuelles. Doc Lab Geol Facl Sci Lyon. 79:1–1185.
Habinger SG, Chavasseau O, Jaeger JJ, Chaimanee Y, Soe AN, Sein C, Bocherens H. 2022. Evolutionary ecology of Miocene hominoid primates in Southeast Asia. Sci Rep. 12(1):1–12. doi: 10.1038/s41598-022-15574-z.
Handa N, Nakatsukasa M, Kunimatsu Y, Nakaya H. 2018. *Brachypotherium* (Perissodactyla, Rhinocerotidae) from the late Miocene of Samburu Hills, Kenya. Geobios. 51(5):391–399. doi: 10.1016/j.geobios.2018.08.003.
Handa N, Nishioka Y, Duangkrayom J, Jintasakul P. 2021. *Brachypotherium perimense* (Perissodactyla, Rhinocerotidae) from the Miocene of Nakhon Ratchasima, Northeastern Thailand, with comments on fossil records of *Brachypotherium*. Hist Biol. 33(9):1642–1660. doi: 10.1080/08912963.2020.1723578.
Heissig K. 1972. Paläontologische und geologische Untersuchungen im Tertiär von Pakistan. V. Rhinocerotidae (Mamm.) aus den unteren und mittleren Siwalik-Schichten. Abh Bayer Akad Wiss Math-Naturwiss Kl. 152:1–112.
Heissig K. 1975. Rhinocerotidae aus dem jungtertiär Anatoliens. Geolog Jahr Reihe B. 15:145–151.
Heissig K. 1999. Family Rhinocerotidae. In: Rössner GE, Heissig K, editors. The Miocene land mammals of Europe. Munich: Verlag Dr. F. Pfeil; p. 175–188.
Hooijer DA. 1963. Miocene Mammalia of Congo. Mus R Afr Cent Ann Sci Géol. 46:1–77.
Hooijer DA. 1966. Fossil Mammals of Africa No. 21: Miocene Rhinoceroses of East Africa. Br Mus Publ. 13(2):119–190.
Hooijer DA, Patterson B. 1972. Rhinoceroses from the Pliocene of northwestern Kenya. Bull Mus Comp Zool. 144(1):1–26.
Hünerman KA. 1989. Die Nashornskelette (*Aceratherium incisivum* Kaup 1832) aus dem Jungtertiär vom Höwenegg im Hegau (Südwestdeutschland). Andrias. 6(1):128.
Iqbal M, Maqsood S, Khan MA, Khan AQ, Khan Sulehria AQ, Nayyer AQ, Akhtar M. 2013. New remains of *Brachypotherium* (Mammalia, Rhinocerotidae) from Dhok Pathan Formation of Middle Siwaliks, Northern Pakistan. Biologia (Pak). 59(2):245–249.
Jin CZ, Liu JY. 2009. Paleolithic site – the Renzidong Cave, Fanchang, Anhui, China. Beijing. [Chin Engl summary] Sci Press. 439.
Khan AM. 2009. Taxonomy and distribution of rhinoceroses from the Siwalik Hills of Pakistan [dissertation]. Pakistan: University of the Punjab Lahore.
Khan AM, Habib A, Khan MA, Ali M, Akhtar M. 2010. New remains of *Brachypotherium fatehjangense* from the lower Siwalik Hills, Punjab, Pakistan. J Anim Plant Sci. 20(2):79–82.
Koufos GD, Kostopoulos DS. 2013. Apr. First report of *Brachypotherium* Roger, 1904 (Rhinocerotidae, Mammalia) in the Middle Miocene of Greece. Geodiversitas. 35(3):629–641. doi: 10.5252/g2013n3a6.
Laurie WA, Lang EM, Groves CP. 1983. *Rhinoceros unicornis*. Mamm Species. 211(211):1–16. doi: 10.2307/3504002.
Li SJ, Deng T. 2023. Restudy of Rhinocerotini fossils from the Miocene Jiulongkou Fauna of China. Vertebra PalAsiat. 61(3):198–211.
Longuet M, Thein Z-MM, Htike T, Nyein MT, Takai M. 2023. New fossil remains of Rhinocerotidae (Perissodactyla) from the early Late Miocene, Tebingan Area central Myanmar. Hist Biol. p(8):1468–1481. doi: 10.1080/08912963.2023.2218873.
Lu XK, Deng T, Ji XP. 2021. Postcranial bones of *Acerorhinus yuanmouensis* from the Late Miocene of the Yuanmou Basin, China, and body reconstruction. Chin Sci Bull. 66:1516–1526 (in Chinese). 10.1360/TB-2020-0743.
Métais G, Antoine PO, Baqri SH, Crochet JY, De Franceschi D, Marivaux L, Welcomme JL. 2009. Lithofacies, depositional environments, regional biostratigraphy and age of the Chitarwata Formation in the Bugti Hills, Balochistan, Pakistan. J Asian Earth Sci. 34(2):154–167. doi: 10.1016/j.jseaes.2008.04.006.
MorphoSource. 2013. Duke University Trinity College of Arts and Sciences. https://www.morphosource.org/.
Nowak RM. 1991. Walker's Mammals of the World. Fifth Edition). Vol 2. 1304–1321. Baltimore: Johns Hopkins University Press.
Pandolfi L, Antoine PO, Bukhsianidze M, Lordkipanidze D, Rook L. 2021. Northern Eurasian rhinocerotines (Mammalia, Perissodactyla) by the Pliocene–Pleistocene transition: phylogeny and historical biogeography. J Syst Palaeontol. 19(15):1031–1057. doi: 10.1080/14772019.2021.1995907.
Pandolfi L, Maiorino L. 2016. Reassessment of the largest Pleistocene rhinocerotine *Rhinoceros platyrhinus* (Mammalia, Rhinocerotidae) from the Upper Siwaliks (Siwalik Hills, India). J vertebr Paleontol. 36(2):e1071266. doi: 10.1080/02724634.2015.1071266.
Pandolfi L, Rook L. 2019. The latest Miocene Rhinocerotidae from Sahabi (Libya). C R Palevol. 18(4):442–448. doi: 10.1016/j.crpv.2019.03.002.
Pandolfi L, Tagliacozzo A. 2015. *Stephanorhinus hemitoechus* (Mammalia, Rhinocerotidae) from the late Pleistocene of Valle Radice (Sora, Central Italy) and re-evaluation of the morphometric variability of the species in Europe. Geobios. 48(2):169–191. doi: 10.1016/j.geobios.2015.02.002.
Pilgrim GE. 1912. The vertebrate fauna of the Gaj series in the Bugti hills and the Punjab. Mem Geol Surv India. 4:1–83.
Prothero DR. 2005. The Evolution of North American Rhinoceroses 1–218. Cambridge: Cambridge University Press.

Prothero DR, Guérin C, Manning E. 1989. The history of the Rhinocerotoidea. Evol perissodactyls. 15:321–340.
Prothero DR, Schoch RM. 2002. Horn, Tusk and Flippers 1–311. Baltimore and London: Johns Hopkins University Press.
Rafeh A, Khan AM, Ahmad RM, Iqbal M, Akhtar M. 2020. Systematic and paleoecological study of the new remains of *Brachypotherium* (Rhinocerotidae) from the Middle Miocene Siwaliks (Pakistan). Arab J Geosci. 13(14):1–20. doi: 10.1007/s12517-020-05657-4.
Ringström T. 1924. Nashörner der Hipparion-Fauna Nord-Chinas. Palaeontol Sin Ser C. 1(4):1–159.
Samiullah K, Draz O, Yasin R, Rasool B, Muhammad Ishaq H, Haris Aziz M, Mehroz Fazal R, Naz S, Raza T, Niazi R. 2021. New discovery of *Hipparion theobaldi* skull from the Late Miocene of Padhri, District Jhelum, Punjab, Pakistan and Associated Mammalian fossil assemblage. Act Geol Sin Engl Ed. 96(4):1150–1165. doi: 10.1111/1755-6724.14711.
Saña AB. 2008. Phylogénie du rhinocérotidé *Diaceratherium* Dietrich, 1931 (Mammalia, Perissodactyla). [master's thesis]. Bibliothèque cantonale jurassienne.
Sein C. 2020. A New *Stegolophodon* (Proboscidea, Mammalia) from the Irrawaddy Formation of Myanmar. Op J Geol. 10(8):863–873. doi: 10.4236/ojg.2020.108039.
Sein C, Thein T. 2013. A New Record of *Chalicotherium* from the Irrawaddy Formation in Migyaungye Area, Magway Region. Univ Res J. 6(5):207–218.
Stamp LD. 1922. An outline of the tertiary geology of Burma. Geol Mag. 59 (11):481–501. doi: 10.1017/S001675680010915X.
Suraprasit K, Jaeger JJ, Chaimanee Y, Chavasseau O, Yamee C, Tian P, Panha S. 2016. The Middle Pleistocene vertebrate fauna from Khok Sung (Nakhon Ratchasima, Thailand): biochronological and paleobiogeographical implications. ZooKeys. 613:1–157. doi: 10.3897/zookeys.613.8309.
Takai M, Htike T, Thein Z-MM, Soe AN, Maung M, Tsubamoto T, Egi N, Nishimura TD, Nishioka Y. 2015. First discovery of colobine fossils from the Late Miocene/Early Pliocene in central Myanmar. J Hum Evol. 84:1–15. doi: 10.1016/j.jhevol.2015.04.003.
Takai M, Nyo K, Kono RT, Htike T, Kusuhashi N, Thein Z-MM. 2021. New hominoid mandible from the early Late Miocene Irrawaddy Formation in Tebingan area, central Myanmar. Anthropol Sci. 129(1):87–98. doi: 10.1537/ase.2012131.
Thein Z-MM, Htike T, Tsubamoto T, Takai M, Egi N, Maung M. 2006. Early Pleistocene Javan rhinoceros from the Irrawaddy Formation, Myanmar. Asian Paleoprimatol. 4:197–204.
Thein Z-MM, Masanaru T, Tsubamoto T, Htike T, Egi N, Maung M. 2008. A new species of *Dicerorhinus* (Rhinocerotidae) from the Plio-Pleistocene of Myanmar. Palaeontology. 51(6):1419–1433.
Thein Z-MM, Takai M, Tsubamoto T, Egi N, Htike T, Nishimura T, Maung M, Win Z. 2010. A review of fossil rhinoceroses from the Neogene of Myanmar with description of new specimens from the Irrawaddy sediments. J Asian Earth Sci. 37(2):154–165. doi: 10.1016/j.jseaes.2009.08.009.
Thein Z-MM, Takai M, Uno H, Wynn JG, Egi N, Tsubamoto T, Htike T, Soe AN, Maung M, Nishimura T, et al. 2011. Stable isotope analysis of the tooth enamel of Chaingzauk mammalian fauna (late Neogene, Myanmar) and its implication to paleoenvironment and paleogeography. Palaeogeogr, Palaeoclimatol, Palaeoeco. 300(1–4):11–22. doi: 10.1016/j.palaeo.2010.11.016.
Tong HW. 2012. Evolution of the non-Coelodonta dicerorhine lineage in China. C R Palevol. 11(8):555–562. doi: 10.1016/j.crpv.2012.06.002.
Tong HW, Guérin C. 2009. Early Pleistocene *Dicerorhinus sumatrensis* remains from the Liucheng *Gigantopithecus* Cave, Guangxi, China. Geobios. 42 (4):525–539. doi: 10.1016/j.geobios.2009.02.001.
Yan Y, Wang Y, Jin C, Mead JI. 2014. New remains of *Rhinoceros* (Rhinocerotidae, Perissodactyla, Mammalia) associated with *Gigantopithecus blacki* from the Early Pleistocene Yanliang Cave, Fusui, South China. Quat Int. 354:110–121. doi: 10.1016/j.quaint.2014.01.004.
Yan Y, Wang Y, Zhu M, Chen S, Qin D, Jin C. 2016. New early Pleistocene perissodactyl remains associated with *Gigantopithecus* from Yangliang Cave, Guangxi of southern China. Hist Biol. 28(1–2):237–251. doi: 10.1080/08912963.2015.1028930.